

Special Section:

Forum for Arctic Modeling and Observational Synthesis (FAMOS)
2: Beaufort Gyre phenomenon

Key Points:

- A 1-D model is employed to study a weakly turbulent double-diffusive staircase
- There is a critical level of turbulence above which a staircase cannot form
- Heat fluxes through a staircase may decrease with increased turbulence

Correspondence to:

N. C. Shibley,
nicole.shibley@yale.edu

Citation:

Shibley, N. C., & Timmermans, M.-L. (2019). The formation of double-diffusive layers in a weakly turbulent environment. *Journal of Geophysical Research: Oceans*, 124. <https://doi.org/10.1029/2018JC014625>

Received 1 OCT 2018

Accepted 12 FEB 2019

Accepted article online 15 FEB 2019

The Formation of Double-Diffusive Layers in a Weakly Turbulent Environment

N. C. Shibley¹ and M.-L. Timmermans¹

¹Department of Geology and Geophysics, Yale University, New Haven, CT, USA

Abstract Double-diffusive stratification in the ocean is characterized by staircase structures consisting of mixed layers separated by high-gradient interfaces in temperature and salinity. These double-diffusive layers, which flux heat vertically, are observed over a vast region of the Arctic Ocean at the top boundary of the relatively warm and salty Atlantic water layer. In one formalism for the origin of double-diffusive layers, staircase formation arises when a heat source is applied at the base of water that is stably stratified in salinity. This framework is extended to consider the effect of intermittent shear-driven turbulence on diffusive-convective staircase formation. One-dimensional numerical model results indicate that there is a critical level of intermittent turbulence above which a staircase cannot form. This is framed in terms of a critical diffusivity ratio (ratio of effective salinity diffusivity to effective thermal diffusivity) that cannot be exceeded for a staircase to persist. This critical ratio is not a universal constant but rather differs for each staircase. Model results further indicate that layer thicknesses decrease with height in a staircase, with the variation in thickness over a staircase being more pronounced in the presence of intermittent turbulence. Finally, results suggest that increased diffusivity ratios lead to decreased heat fluxes across interfaces; if a staircase is subject to intermittent turbulence levels (below the critical level), vertical heat fluxes will be smaller than in the absence of shear-driven turbulence. Findings are related to double-diffusive staircases, and associated heat fluxes, in the weakly turbulent Arctic Ocean.

Plain Language Summary Double diffusion is a type of convective mixing process that may arise in the oceans where temperature and salinity determine density gradients. Active double diffusion manifests as stacked well-mixed water layers, forming a staircase structure. The Arctic Ocean exhibits a notable double-diffusive staircase which indicates how deep-ocean heat is mixed vertically toward the sea ice. In this study, we examine how this double-diffusive heat transport may be influenced by mechanical mixing, or turbulence, such as that driven by winds and waves. We find that below a threshold level of turbulence, the vertical transport of heat through the staircase may be reduced as turbulence increases. However, we find that above this threshold level of turbulence, double diffusion can no longer operate to generate a well-formed staircase. Results contribute to understanding how turbulence affects vertical heat transport in a changing Arctic Ocean that may experience higher wind-driven mixing as sea ice continues to retreat.

1. Introduction

1.1. Mechanisms of Double Diffusion

Double diffusion is a type of heat transfer that can exist in regions of the ocean when the vertical gradient of either temperature or salinity is destabilizing (e.g., Schmitt, 1994; Turner & Stommel, 1964; Turner, 1965). There are two modes of double diffusion: salt fingers and diffusive convection (e.g., Kelley et al., 2003). In this paper, we consider only diffusive convection, the mode of heat transfer that can occur when the water column is stably stratified with respect to salinity, while the temperature stratification is destabilizing. A density ratio defined as $R_\rho = (\beta \frac{\partial S}{\partial z}) / (\alpha \frac{\partial T}{\partial z})$ quantifies the ratio of contributions of salinity S and temperature T to density ρ . Here $\beta = \rho_0^{-1} \partial \rho / \partial S$ is the coefficient of haline contraction, $\alpha = -\rho_0^{-1} \partial \rho / \partial T$ is the coefficient of thermal expansion, ρ_0 is a reference density, and z is the vertical coordinate. In general, in an ocean setting where diffusive convection is active, $1 < R_\rho \leq 10$ (e.g., Kelley et al., 2003).

Diffusive convection in the ocean is characterized by staircase structures consisting of mixed layers separated by high-gradient interfaces in temperature and salinity (e.g., Radko, 2013; Turner, 1965; Timmermans et al., 2008). Interfaces are composed of stable cores bounded by temperature and salinity boundary layers

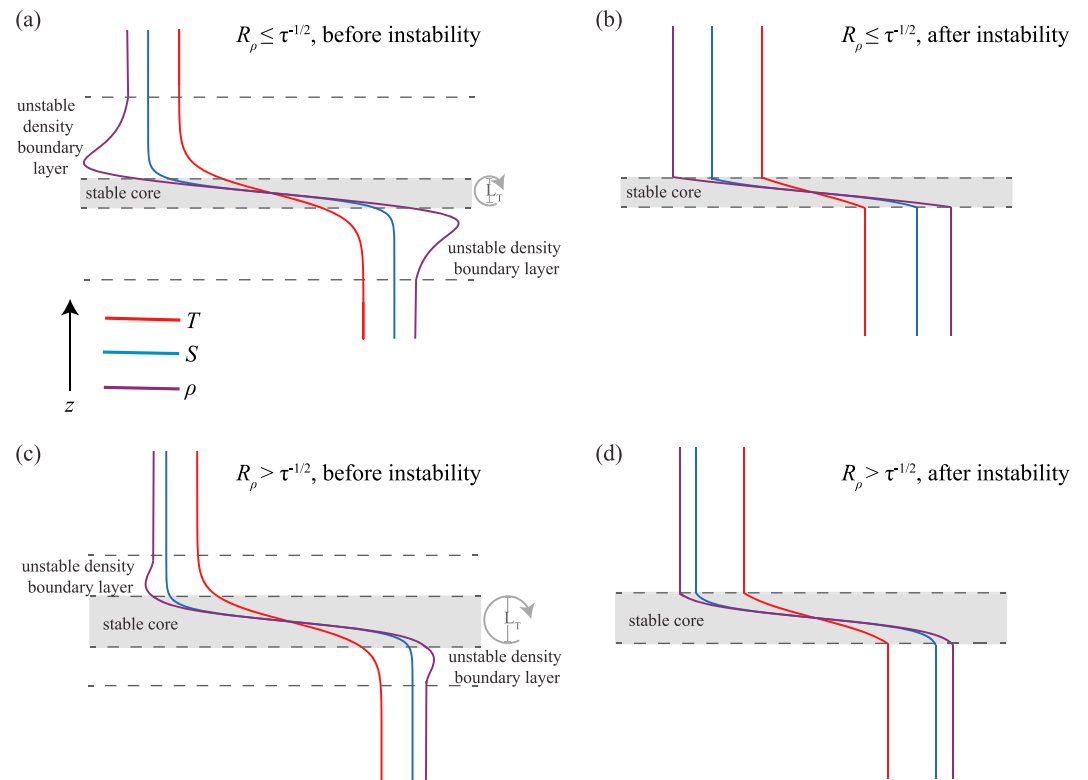


Figure 1. Schematic of diffusive-convective interface boundary layer profiles of temperature (red), salinity (blue), and density (purple) for $R_\rho \leq \tau^{-1/2}$ (a) before and (b) after the boundary layer overturns. Diffusive-convective boundary layer profiles for $R_\rho > \tau^{-1/2}$ (c) before and (d) after the boundary layer overturns. The stable core is shaded grey, and the unstable density boundary layers are labeled. Turbulent overturns are shown by the grey arrows in (a) and (c), with the Thorpe scale L_T labeled.

(e.g., Carpenter et al., 2012b; Linden & Shirtcliffe, 1978; Worster, 2004; Figure 1). A thermal boundary layer (whose thickness depends on the molecular diffusivity of heat, $\kappa_T = 1.4 \times 10^{-7} \text{ m}^2/\text{s}$) is thicker than a salinity boundary layer (governed by the molecular diffusivity of salt, $\kappa_S = 1.1 \times 10^{-9} \text{ m}^2/\text{s}$). These temperature and salinity boundary layers give rise to a density boundary layer (whose shape depends on R_ρ , to be discussed later) which becomes increasingly unstable over time (e.g., Huppert & Linden, 1979; Radko, 2013; Turner, 1968; Veronis, 1965; Figure 1). Convection is driven by instability of the boundary layers (see Carpenter et al., 2012b), which may be characterized by a critical boundary layer Rayleigh number of order 10^2 – 10^4 (Carpenter et al., 2012a; Linden & Shirtcliffe, 1978; Worster, 2004).

1.2. Arctic Observations of Diffusive Convection

Diffusive convection has been observed in many regions in the World's oceans and lakes, perhaps most notably in the Arctic Ocean (Guthrie et al., 2015; Neal et al., 1969; Padman & Dillon, 1987, 1988; Polyakov et al., 2012; Sirevaag & Fer, 2012; Shibley et al., 2017; Timmermans et al., 2003, 2008; Turner, 2010). In the Arctic Ocean, the relatively warm and salty Atlantic water layer underlies relatively cooler and fresher water layers. The resulting vertical gradients in temperature (destabilizing) and salinity (stabilizing) give rise to a diffusive-convective staircase (e.g., Polyakov et al., 2012; Timmermans et al., 2008; Figures 2a and 2b). Vertical heat fluxes through the staircase range from $O(0.01\text{--}0.1) \text{ W/m}^2$ in the interior of the Arctic Basin away from boundary regions (Guthrie et al., 2015; Padman & Dillon, 1987; Shibley et al., 2017; Timmermans et al., 2008) to $O(1) \text{ W/m}^2$ near the Laptev Sea slope (Lenn et al., 2009; Polyakov et al., 2012). Results here are interpreted and discussed in context with the Arctic Ocean diffusive-convective staircase associated with the Atlantic water layer.

In an Arctic-wide analysis of Ice-Tethered Profiler (ITP) data, Shibley et al. (2017) characterized regional differences in properties of the diffusive-convective staircase, including mixed-layer thicknesses, interface thicknesses, and temperature and salinity jumps across interfaces, across the Arctic Basin. Further, they

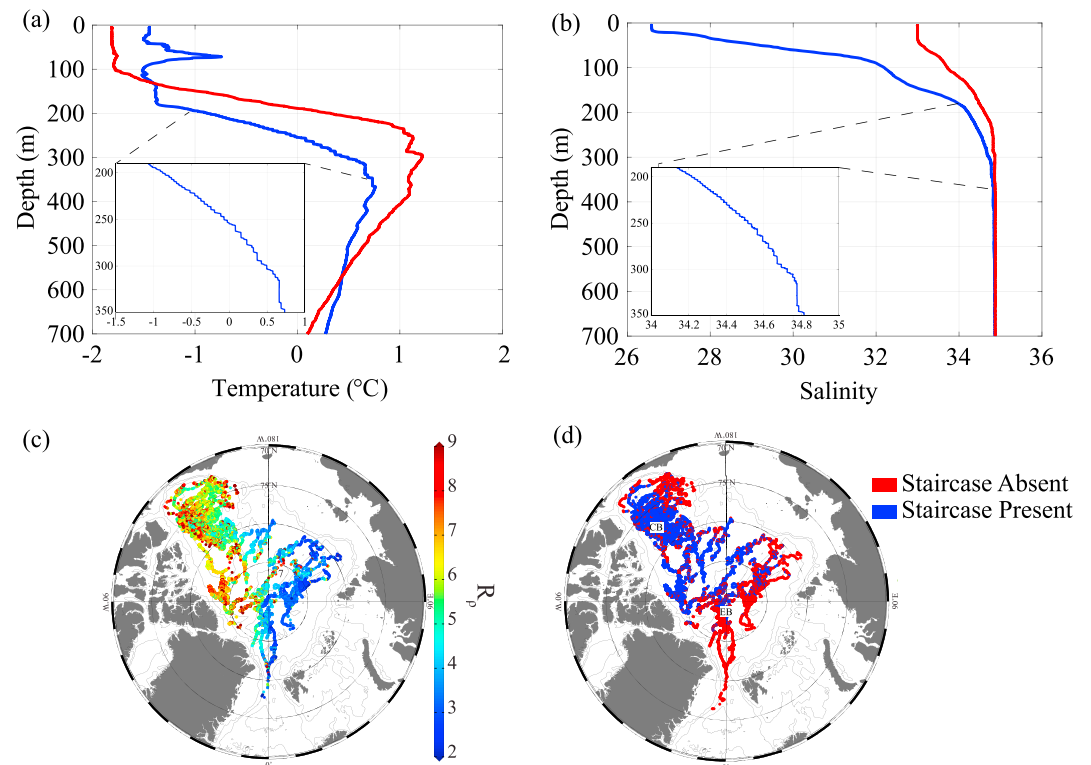


Figure 2. Ice-Tethered Profiler measurements. (a) Temperature-depth profiles from the Canadian Basin (CB, blue) and the Eurasian Basin (EB, red). (b) Salinity-depth profiles from the Canadian Basin (blue) and Eurasian Basin (red). Insets in (a) and (b) show the diffusive-convective staircase at the top boundary of the Atlantic water layer. Profile locations indicated by CB, EB in panel (d). (c) Map of dimensional R_ρ in the Arctic Basin, where R_ρ is computed as $R_\rho = \beta \frac{\partial S}{\partial z} / \alpha \frac{\partial T}{\partial z}$ over an approximately linear 50-m segment in the thermocline. (d) Map showing the presence (blue) or absence (red) of a well-formed staircase structure across the Arctic Basin. Figure modified from Shibley et al. (2017).

quantify the density ratio R_ρ over a 50-m depth segment of the thermocline and find values in the range $1 < R_\rho \leq 10$ across the Arctic (Figure 2c). Shibley et al. (2017) find that while staircases are widely present in the Makarov and central Canada basins, they are absent around more energetic boundary regions and in parts of the Eurasian Basin, even though the range of R_ρ is similar in both regions (Shibley et al., 2017; Figure 2d). This suggests that although the water column is characterized by a stratification that is amenable to diffusive convection, other factors may prevent staircase formation.

1.3. Double Diffusion and Shear-Driven Turbulence

A possible explanation for the absence of a staircase in regions where we would otherwise expect them (based on the local value of R_ρ) is the presence of shear-driven turbulence. Staircases may only exist where this turbulence is sufficiently weak (or intermittent) so as not to destroy a staircase structure (e.g., Guthrie et al., 2017; Kunze, 1990; Padman, 1994; Shaw & Stanton, 2014). Based on microstructure measurements from the Yermak Plateau, Padman (1994) reports staircases only in regions with background shear less than around 0.004 s^{-1} . For these regions, he suggests that the presence of a staircase may give rise to enhanced decay of shear as a result of convection in layers. In general, shear is focused at staircase interfaces, which may lead to increased heat, salt, and momentum fluxes through interfaces due to increased entrainment (see Padman, 1994). The absence of diffusive-convective staircases has been linked to larger-than-molecular diffusivities in both the Chukchi Borderlands and the Amundsen Basin, where the inferred turbulent thermal diffusivities were $O(10^{-5}) \text{ m}^2/\text{s}$ compared to molecular values of $O(10^{-7}) \text{ m}^2/\text{s}$ (Guthrie et al., 2017; Shaw & Stanton, 2014). Here we explore the effects of shear-driven turbulence on a diffusive-convective staircase and related vertical heat fluxes. We note that this may be of particular relevance to a changing Arctic Ocean subject to sea ice decline and subsequent increased wind-energy input to an upper ocean characterized by more expansive open-water regions (see, e.g., Carmack et al., 2015; Kwok & Untersteiner, 2011).

1.4. Effective Diffusivities for Heat and Salt Across an Interface

To consider how the presence of weak (or intermittent) shear-driven turbulence may affect double diffusion at a staircase interface, we introduce effective diffusivities K_T and K_S for heat and salt, respectively. K_T and K_S take values that are larger than their molecular counterparts; the formalism is analogous to the concept of *differential diffusivities* described by Gargett (2003). Here intermittent means short-lived compared to a time series of staircase observations, similar to the work of Wells and Griffiths (2003) who studied how salt fingers (the mode of double diffusion active where temperature and salinity both decrease with depth) are affected by intermittent turbulence in laboratory experiments.

Consider a turbulent fluctuation of vertical scale smaller than the thickness of an interface core. This turbulent fluctuation transfers both heat and salt vertically across an interface; turbulent diffusivities for heat and salt are equal. The Thorpe scale (L_T) characterizes the vertical length scale of a turbulent overturn (Thorpe, 1977) in the stratified interface core. This scale must be less than the thickness of the interface (so as not to destroy the interface entirely), which corresponds to an upper bound on turbulent diffusivity κ^{turb} (see Timmermans et al., 2003, who applied this reasoning to a diffusive-convective interface; Figures 1a and 1c). For L_T being the maximum vertical scale of a turbulent overturn, the upper bound on κ^{turb} is given by $\kappa^{\text{turb}} = 0.1NL_T^2$, where $N = [(-g/\rho_0)d\rho/dz]^{1/2}$ is the buoyancy frequency characterizing the interface (Dillon, 1982; Thorpe, 1977). For a typical core thickness of $O(10)$ cm (e.g., Timmermans et al., 2008), and $N \approx 10^{-3} \text{ s}^{-1}$, $\kappa^{\text{turb}} \approx 10^{-6} \text{ m}^2/\text{s}$. This is of similar magnitude to diffusivities inferred from microstructure measurements in staircase regions in the Arctic Ocean (e.g., Guthrie et al., 2017). Therefore, when shear-driven turbulence intermittently affects an interface core, resulting in instantaneous $\kappa^{\text{turb}} = 10^{-6} \text{ m}^2/\text{s}$, heat is transported 10 times faster than it is by molecular diffusion, while salt is transported 1,000 times faster than by molecular diffusion.

A weighted-average diffusivity ratio describing the contributions of molecular diffusion and shear-driven mixing at an interface may be defined in terms of κ_T , κ_S , κ^{turb} , and a relative percentage of time P_T that mixing is dominated by shear-driven turbulence as follows:

$$\tau \equiv \frac{K_S}{K_T} = \frac{(1 - P_T)\kappa_S + P_T\kappa^{\text{turb}}}{(1 - P_T)\kappa_T + P_T\kappa^{\text{turb}}}. \quad (1)$$

This diffusivity ratio is analogous to the formulation presented in St. Laurent and Schmitt (1999) and Inoue et al. (2007). St. Laurent and Schmitt (1999) deduce active turbulence in 52% to 95% of measurements in a region of the North Atlantic where double diffusion (here, salt fingers) is also active, suggesting $P_T = 0.52$ – 0.95 in this region. Similarly, Inoue et al. (2007) infer $P_T \approx 0.69$ in the Kuroshio region off the east coast of Japan. Thus, we may examine intermittent turbulence in an ocean setting by considering the effects of increasing τ , which can then be related to P_T via (1), above its value in the absence of turbulence (i.e., $\tau = 0.01$ corresponding to $P_T = 0$).

1.5. Studies of Layer Formation

Past studies have examined the mechanisms that govern the formation and evolution of double-diffusive staircases in both one- and two-dimensional systems (Huppert & Linden, 1979; Turner, 1968; Radko, 2003, 2005, 2007, 2014). These have included laboratory experiments and 1-D models where heat is applied to the bottom of water with a stable linear salinity gradient which then forms a layered system of diffusive convection (e.g., Huppert & Linden, 1979; Turner, 1965, 1968). A 2-D system by way of horizontal thermohaline intrusions which perturb linear gradients in temperature and salinity may also lead to a staircase structure (Bebieva & Timmermans, 2017; Merryfield, 2000). Finally, a recent study has described the formation of staircases where the presence of shear in a stably stratified system allows perturbations to buoyancy to grow, leading to a layered system (Radko, 2016).

Here we consider the simplest 1-D setup of a stable salinity gradient heated at its base (following Huppert & Linden, 1979) to examine the influence of intermittent turbulence on staircase formation and heat fluxes. In the next section, we describe the 1-D model of staircase development. Section 3 extends the model to explore the effects of intermittent turbulence, where shear-driven turbulence is represented by diffusivity ratios above molecular. Section 4 considers model results in context with Arctic observations. Section 5 summarizes and discusses the results.

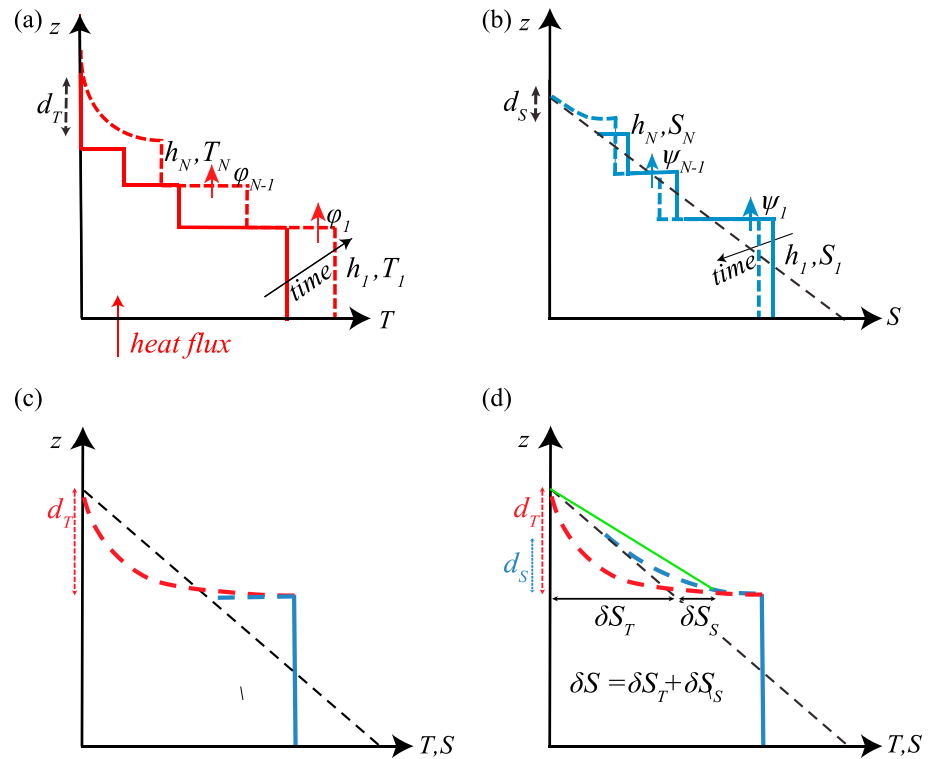


Figure 3. Schematic of the 1-D model setup showing (a) dimensionless temperature-depth and (b) salinity-depth profiles of the growing staircase. A heat flux is applied to the bottom of the staircase. h_N , T_N , and S_N are the thickness, temperature, and salinity of the top growing layer, and h_1 , T_1 , and S_1 are the thickness, temperature, and salinity of the first layer. ϕ_i and ψ_i are the heat and salt fluxes through the i th interface. (c) Schematic of the boundary layer across the top interface in the 1-D model of Huppert and Linden (1979) with $\tau = 0$. (d) Schematic of the salinity difference approximation used in the Rayleigh-number formulation for $\tau > 0$. δS_T is the salinity jump across the temperature boundary layer, and δS_S is the approximate salinity jump across the salinity boundary layer. d_T and d_S are the thicknesses of the thermal boundary and salinity boundary layers, respectively. The salinity boundary layer is shown by the dashed blue line, and the approximate salinity gradient across the thermal boundary layer is shown by the green line. The dashed black line shows the background salinity gradient prior to staircase formation. δS is the total approximate salinity jump across the thickness d_T considered in the Rayleigh-number derivation.

2. One-Dimensional Model: Stable Salinity Gradient Heated From Below

2.1. Model Setup

The formation of a diffusive-convective staircase is examined by modifying the 1-D model of Turner (1968) and Huppert and Linden (1979) to account for finite values of τ from 0. Huppert and Linden (1979) formulate the model in the absence of turbulence and for $\tau = 0$ (i.e., there is no diffusion of salt, only temperature). The setup is a stable salinity gradient subject to a constant heat flux at the bottom, which forms an N -layer system (Figures 3a and 3b). This basal boundary condition of a constant heat flux may be applicable in the Arctic setting, where the vast Atlantic water layer heat reservoir could provide a nearly constant heat flux upward. Heat and salt fluxes across each interface in the system drive the evolution of adjacent layers, governed by conservation of heat and salt. There is no heat loss from the system; the entire basal heat flux goes into increasing the staircase in total height and temperature over time (i.e., the heat content integrated vertically over the staircase structure is only a function of the constant basal heat flux and time). This is consistent with heat fluxes across interfaces that decrease with height in the staircase. The thickness of a fully formed layer remains constant, and only its temperature and salinity change in time. The uppermost layer (the N th layer) is the only one which is not yet fully formed and continues to grow in thickness. While fully formed layers do not become thicker over time, two layers can merge (to form a new layer with thickness equal to the sum of the originating layer thicknesses) once the interface separating them is characterized by $R_\rho = 1$. After layer-merging takes place, the temperature and salinity of the new layer are equal to the thickness-weighted averages of the temperature and salinity of the original layers.

The evolution of the N th layer in the 1-D system is governed by the formation of a thermal boundary layer across its top (Figure 3c). This layer grows in thickness and temperature until the onset of diffusive-convective instability, which takes place when the Rayleigh number, characterizing the influence of buoyancy to viscosity and diffusion, exceeds a critical value (see Huppert & Linden, 1979).

The Rayleigh number, Ra , characterizing the boundary layer at the top of the N th layer is derived from a linear stability analysis of a perturbation to the boundary layer temperature gradient (assumed to be linear) and the ambient salinity gradient (Huppert & Linden, 1979; Veronis, 1965). As heat is diffused across the top of the N th layer, the Ra (defined in the next section) increases. When $Ra = Ra_c = 10,000$ (Huppert & Linden, 1979), the boundary layer becomes unstable and overturns. At this point, the layer ceases to grow in thickness, and a new layer at the top of the staircase is formed. The initial conditions governing the temperature, salinity, and thickness of this newly formed layer are as follows: (1) The amount of heat in the new layer is set by the amount of heat in the boundary layer immediately prior to its overturn, (2) the boundary layer mixes up some amount of salinity related only to the background stratification, which sets the salinity of the new layer, and (3) there is no density jump across the top of the new layer. If the system has only one layer, the conditions describing the thickness, temperature, and salinity of this layer are those described by Turner (1968).

2.2. Governing Equations and Parameters

The N -layer diffusive-convective system formulated by Huppert and Linden (1979) is described here. Variables are nondimensionalized as follows, where hats denote dimensionless variables (time \hat{t} , depth \hat{z} , temperature \hat{T} , and salinity \hat{S}):

$$\hat{t} = S_*^{1/2} t \quad (2)$$

$$\hat{z} = H_*^{-1/2} S_*^{3/4} z \quad (3)$$

$$\hat{T} = H_*^{-1/2} S_*^{-1/4} (\alpha g) T \quad (4)$$

$$\hat{S} = H_*^{-1/2} S_*^{-1/4} (\beta g) S, \quad (5)$$

where $H_* = \alpha g H / \rho c_p$, $S_* = -\frac{1}{2} \beta g d\bar{S}/dz$, H is the heat flux at the bottom, $d\bar{S}/dz$ is the imposed salinity gradient (here, $d\bar{S}/d\hat{z} = -2$), ρ is density, c_p is specific heat, and g is gravity. Hereafter, we drop the hats on dimensionless variables. Conservation of heat and salt, and the assumption that there is no density jump across the top layer (i.e., $R_p = 1$), govern layer evolution; that is,

$$\frac{d}{dt} (h_i T_i) = \phi_{i-1} - \phi_i, \quad (6)$$

$$\frac{d}{dt} (h_i S_i) = \psi_{i-1} - \psi_i, \quad \text{and} \quad (7)$$

$$T_N - S_N - 2 \sum_{i=1}^{i=N} h_i = 0, \quad (8)$$

where ϕ and ψ are the dimensionless interfacial heat and salt fluxes, h is the layer thickness, and subscript i indicates the layer number in the staircase ($i = 1$ refers to the bottom layer). T_N and S_N are the temperature and salinity of the N th layer (see Huppert & Linden, 1979, (3.3)–(3.6), for the complete equations).

The heat flux ϕ through an interface is estimated by a parameterization based on empirical considerations and the assumption that the heat flux across an interface is independent of the layer thickness (Turner, 1965). That is,

$$\phi = 0.32(Q/\sigma)^{1/3} (\Delta T)^{10/3} (\Delta S)^{-2}, \quad (9)$$

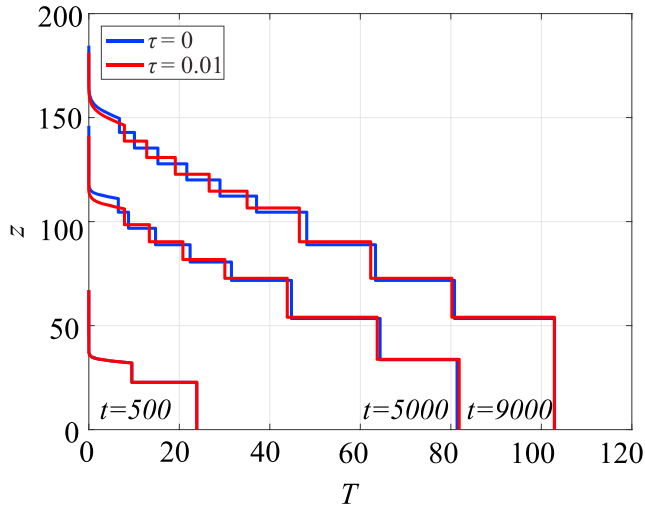


Figure 4. One-dimensional model results showing staircase evolution using flux parameterizations in Huppert and Linden (1979) with $Q = 0.03$ and $\sigma = 7$. Temperature-depth profiles at dimensionless times $t = 500$, $t = 5,000$, and $t = 9,000$ for $\tau = 0$ (blue) and $\tau = 0.01$ (red). Here the base of the staircase is at $z = 0$; the z axis points upward. Variables are dimensionless; see text.

where $\sigma = \nu/\kappa_T$ is the Prandtl number, ν is molecular viscosity, $Q = \kappa_T S_* / H_*$ is proportional to the ratio of the salinity gradient to the bottom heat flux, and ΔT and ΔS are the dimensionless temperature and salinity steps across an interface (Huppert, 1971; Huppert & Linden, 1979; Turner, 1965). The salt flux ψ through an interface is based on empirical relationships that depend on the density ratio and is given by

$$\psi = (1.85 - 0.85R_\rho)\phi, \quad 1 < R_\rho \leq 2 \quad (10)$$

$$\psi = 0.15\phi, \quad 2 \leq R_\rho, \quad (11)$$

where $R_\rho = \Delta S/\Delta T$ (see Huppert, 1971; Huppert & Linden, 1979; Turner, 1965).

The onset of the diffusive-convective oscillatory instability in the boundary layer across the top layer (characterizing the initial instability; see Carpenter et al., 2012b) depends on the Rayleigh number expressed as (Veronis, 1965)

$$Ra = \frac{1}{Q^2 \sigma} \frac{(\sigma + 1)d_T^3}{(\sigma + 1 + \tau)(\frac{\tau}{\sigma} + \tau + 1) - \tau} [\delta T - \delta S(\sigma + \tau)(\sigma + 1)^{-1}]. \quad (12)$$

Here the temperature jump across the thermal boundary layer $\delta T = T_N$, and the salinity jump across the thermal boundary layer $\delta S = 2d_T$, where

d_T is the thickness which would give a linear approximation to the heat content in the thermal boundary layer (Huppert & Linden, 1979; Turner, 1968; Figure 3c). Recall that Huppert and Linden (1979) take $\tau = 0$ in (12).

A fourth-order Runge-Kutta method is used to solve (6)–(8) (cf. Huppert & Linden, 1979). The diffusion equation governing the thermal boundary layer overlying the top mixed layer is solved using a second-order Galerkin method (see Skeel & Berzins, 1990) for 36 grid points at each time step until the critical Rayleigh number is reached. The boundary layer overlying the initial, bottom mixed layer is solved for 2,501 grid points at each time step.

To summarize, Huppert and Linden's (1979) 1-D model runs proceed as follows: After initiation of the run, a single mixed layer at the base of the system begins to grow. When a critical Rayleigh number is reached across the top boundary of this layer, a second overlying layer begins to form. This sequence continues for the duration of the model run. A key result of Huppert and Linden (1979) is that at the end of the model run, the staircase exhibits varying layer thicknesses, with a thick lower layer and thinner upper layers. Further, their 1-D model results show reasonable agreement with their laboratory experiments of a similar setup.

2.3. Incorporating Salinity Diffusion, $\tau = 0.01$

In order to extend the model to account for diffusion of salinity across the upper boundary layer, we relax the assumption of $\tau = 0$ and allow for finite κ_S (for the molecular case in the absence of turbulence, $\tau = 0.01$). This requires modification of the salinity jump across the thermal boundary layer from that described in Huppert and Linden (1979) to allow for the increased salinity jump due to diffusion of salinity across the boundary layer. That is, $\delta S = 2d_T$ becomes $\delta S = 2d_T + 2d_S$ (Figure 3d). For $\tau = 0.01$, $Q = 0.03$ and $\sigma = 7$, we recover the basic staircase structure of Huppert and Linden (1979), and results are effectively indistinguishable from the $\tau = 0$ case (Figure 4). The layer thickness variation, which Huppert and Linden (1979) attribute to frequent mergers of the lowest layer with the adjacent overlying layer, remains an obvious feature of the results. It is of note that we find that this thickness variation exists prior to any merging events in a model run; this is described further in section 4.

3. Extension of the 1-D Model: Intermittent Turbulence

In an extension to the model of Huppert and Linden (1979), we consider how shear-driven turbulence affects both the top boundary layer and the interfaces (in particular, the interface boundary layers) between mixed layers in the staircase (Figure 1). Shear-driven turbulence across the top boundary layer is represented by

a larger-than-molecular τ . Further, we employ heat and salt flux parameterizations that explicitly consider the fundamental interface physics relevant for different values of τ .

Linden and Shirtcliffe (1978) consider an interface where heat and salt are diffused across the interface core into the boundary layers on either side. These boundary layers grow until they reach a critical Rayleigh number, Ra_c , at which point they become convectively unstable and overturn. The entirety of the heat and salt that is diffused across the core is carried into the adjacent mixed layers (Figure 1a). The breakdown of the boundary layers results in a sharpened interface (Figure 1b), and the process starts again. In this case, where the buoyancy diffusion across the interface core is equal to the convective transfer across layers, Linden and Shirtcliffe (1978) formulate heat and salt fluxes across an interface as

$$\phi = \frac{1}{(\pi Ra_c)^{1/3}} \frac{(1 - \tau^{1/2} R_\rho)^{4/3}}{(1 - \tau^{1/2})^{1/3}} \left(\frac{Q}{\sigma} \right)^{1/3} (\Delta T)^{4/3}, \text{ and} \quad (13)$$

$$\psi = \tau^{1/2} \phi. \quad (14)$$

Linden and Shirtcliffe (1978) find that their analysis does not hold for $R_\rho > \tau^{-1/2}$. When this bound on R_ρ is exceeded, diffusive and convective fluxes are not balanced, and different interface physics come into play; Newell (1984) considers this regime.

For $R_\rho > \tau^{-1/2}$, the salinity stratification is so strong that when a density boundary layer becomes unstable and overturns, it leaves behind some salt (i.e., part of the salinity boundary layer). This prevents the interface from sharpening (see Figures 1c and 1d). Instead, the interface grows, governed by the diffusion of salinity (Newell, 1984; Worster, 2004). For this case, considering a scenario absent external forcing, Newell (1984) formulates heat and salt fluxes as

$$\phi = \frac{QR_\rho^{1/3} \Delta T^{4/3} \Delta S^{-1/3}}{2\pi\tau h \ln(R_\rho \tau^{1/2})}, \text{ and} \quad (15)$$

$$\psi = \tau R_\rho \phi, \quad (16)$$

where we take $h = (h_i h_{i+1}) / (h_i + h_{i+1})$ (modified from Newell, 1984). While the parameterization of Newell (1984) considers a run-down scenario, we consider a forced system that is both growing in temperature and transferring heat upward via diffusive convection. However, in the frame of reference of the staircase, we may consider solely the transfer of heat through individual, isolated interfaces, applying Newell's (1984) parameterization at each.

Depending on whether an interface is characterized by $R_\rho \leq \tau^{-1/2}$ or $R_\rho > \tau^{-1/2}$, fluxes in the 1-D model are computed using (13) and (14) or (15) and (16), respectively. Note that Worster (2004) compares the parameterizations of Linden and Shirtcliffe (1978) and Newell (1984) with heat fluxes derived via numerical solutions of the time-dependent equations for a diffusive-convective interface. He finds that the parameterized heat fluxes are reasonably well represented within their respective R_ρ ranges.

We next explore model results in context with Arctic Ocean observations. This allows us to draw comparisons between the 1-D model of stable salinity stratification heated from below and observations at the top boundary of the Atlantic water layer, with the Atlantic water layer warm core providing the basal heat source (see, e.g., Figure 2a).

4. Model Results

4.1. Model Parameters

In the presence of intermittent turbulence, the 1-D model parameters are defined as $\sigma \equiv \nu / K_T$, where ν has both a molecular and an eddy contribution, and $Q \equiv K_T S_* / H_*$. The 1-D model parameters chosen here are $Q = 0.03$ and Prandtl number $\sigma = 7$, equal to those used by Huppert and Linden (1979). These parameters approximately represent the Arctic setting. While molecular values of viscosity and thermal diffusivity in the Arctic Ocean yield $\sigma \approx 13$, values may be in the range $O(0.1 - 1)$ when turbulence is present (Bebieva & Timmermans, 2017; Padman, 1994). Therefore, $\sigma = 7$ is a reasonable choice here. The value chosen for the

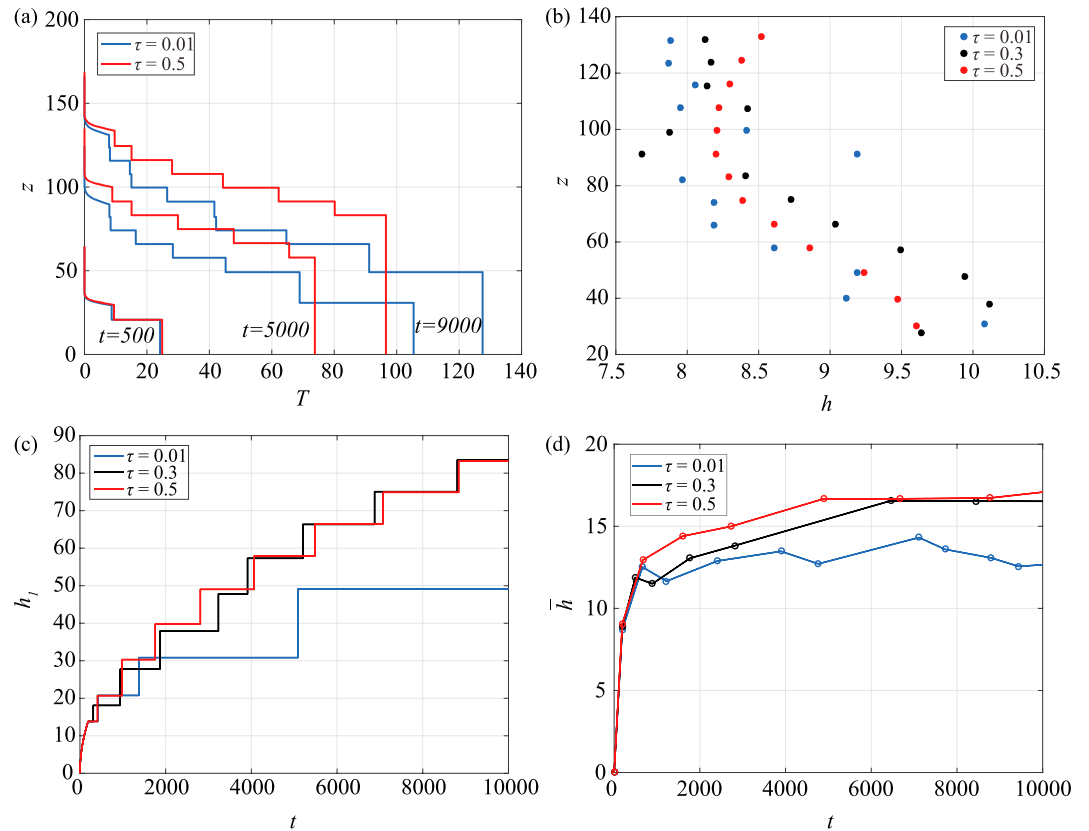


Figure 5. Example 1-D model runs with $Q = 0.03$ and $\sigma = 7$ for a range of τ as noted in the legend where fluxes rely on parameterizations of Linden and Shirtcliffe (1978) ($R_\rho \leq \tau^{-1/2}$) and Newell (1984) ($R_\rho > \tau^{-1/2}$). (a) Temperature-depth profiles for $\tau = 0.01$ (blue), $\tau = 0.5$ (red) at three successive times. $\tau = 0.5$ results exhibit a much thicker bottom layer compared to $\tau = 0.01$. (b) Final thickness h of the top layer in the staircase (with at least two layers) immediately prior to the formation of a new layer, versus its height z in the staircase for three τ values (see legend). Each value of τ exhibits a similar distribution in layer thickness with height. (c) Time series of lower layer thickness h_1 showing much thicker, lower layers for larger τ due to increased merging. (d) Time series of mean layer thickness \bar{h} . Circles indicate the time at which a new layer was formed at the top of the staircase. Variables are dimensionless; see text.

dimensionless ratio $Q \equiv K_T S_* / H_* = K_T \beta \rho c_p (d\bar{S}/dz) / 2\alpha H = 0.03$ is also reasonable for the Arctic setting, assuming K_T varies between $O(10^{-7}-10^{-6})$ m^2/s , $d\bar{S}/dz = O(0.01)$ m^{-1} , $\beta = O(10^{-4})$, $\rho = 10^3$ kg/m^3 , $c_p = O(10^3)$ $\text{J}\cdot\text{kg}^{-1}\cdot\text{K}^{-1}$, and $\alpha = O(10^{-5})$ K^{-1} . Further, $H = O(1 - 10)$ W/m^2 approximates the magnitude of the heat flux sourced from the Atlantic water layer estimated based on observations (e.g., Dewey et al., 1999; Polyakov et al., 2012). For these fixed values of Q and σ , we perform model runs for a range of τ . The general formation and evolution of the staircase structure is similar to the $\tau = 0, 0.01$ cases. We next detail three specific results from the model runs that provide insights into the potential effects of intermittent turbulence.

4.2. Model Result 1: Critical Value of τ

Model results indicate that there exists a maximal value of τ above which a diffusive-convective staircase cannot form. Relatively larger salinity diffusivities compared to thermal diffusivities (i.e., larger values of τ) correspond to increased salt fluxes which stabilize the boundary layer, inhibiting the onset of the diffusive-convective instability. At a critical value of diffusivity ratio, τ_c , the staircase no longer forms because salinity fluxes entirely suppress the vertical transfer of heat (i.e., the boundary layer does not overturn). For $Q = 0.03$ and $\sigma = 7$, model results indicate that the staircase can only evolve for values of $\tau \leq 0.56$. τ_c can be related to the proportion of time shear-driven turbulence affects the water column, giving us an estimate of “how turbulent” a region can be before diffusive convection cannot operate. Note that τ_c differs for each staircase and is not a universal constant. In this sense, the value of τ_c cannot be used to predict a regime and instead characterizes the setting. From (1) with $\kappa^{\text{turb}} = 10^{-6}$ m^2/s , $\tau_c = 0.56$ corresponds to the staircase

being dominated by shear-driven turbulence 15% of the time, $P_T = 15\%$. It may be reasonable to presume that a well-formed staircase will be observed in Arctic observations only when turbulence levels are lower than this.

This basic result may explain why we do not always observe staircases in regions where R_p is amenable to staircase formation (Figures 2c and 2d), and an understanding of τ_c and P_T from model output can be set in context with Arctic observations of the staircase distribution. For example, the finding that a staircase may not exist when P_T exceeds 15% is consistent with hypotheses that the presence of a staircase indicates a sufficiently low level of turbulence (Guthrie et al., 2017; Padman, 1994; Shaw & Stanton, 2014). Both Shaw and Stanton (2014) and Guthrie et al. (2017), for example, do not observe a staircase for values of K_T around $O(10^{-5})$ m²/s, in regions with $R_p \approx 3.5$ –4.5 normally susceptible to diffusive convection. Further, staircases are absent around boundary regions (Figure 2d; Shibley et al., 2017), where the rate of viscous dissipation of kinetic energy has been shown to be larger than in regions where the diffusive-convective staircase is observed (Rippeth et al., 2015). Rippeth et al. (2015) propose that this may be due to enhanced turbulence associated with seafloor topography. It will be useful to test the bounds inferred from the 1-D model through analyses of microstructure to infer turbulent mixing levels as they relate to regional distributions of a well-formed staircase.

We next consider the sensitivity of τ_c to varying σ and Q . Varying the value of σ from 1 to 13 (for fixed $Q = 0.03$) yields values of τ_c that differ by less than 10%. On the other hand, the value of τ_c is more sensitive to variations in the basal heat flux. Varying Q within the range $O(0.01$ – $0.1)$ (corresponding to H in the range $O(10$ – $1)$ W/m², and $K_T = O(10^{-7}$ – $10^{-6})$ m²/s) for fixed $\sigma = 7$ yields values of τ_c spanning 0.01–0.95 (for $Q = 0.06$ – 0.02). For a sufficiently small basal heat flux (i.e., large Q , where the exact value depends on the choice of σ), any level of intermittent turbulence will prevent staircase formation. For a sufficiently large heat flux (small Q), diffusive convection can persist in the presence of higher mixing levels. Taking $\sigma < 7$ yields a larger range of Q over which a staircase can persist within the range $O(0.01$ – $0.1)$. This indicates that if the fluid is less viscous or if diffusion is faster, a smaller heat flux can generate layers in the presence of turbulence; the opposite is true for $7 < \sigma < 13$. Additional model runs for different values of σ and Q (over ranges of $O(1$ – $10)$ and $O(0.01$ – $0.1)$, respectively) produced similar results to those described next.

4.3. Model Result 2: Variation in Layer Thickness With Depth in the Staircase

Model results show a layer thickness variation with depth for all $\tau \leq \tau_c$, with thicker, lower layers and thinner, upper layers (Figures 5a and 5b; cf. Huppert & Linden, 1979), as described earlier for the $\tau = 0, 0.01$ cases. This may be explained as follows. The heat content of a newly forming layer increases in time via both increases in its thickness, h , and its temperature (i.e., increases in δT across the top of the layer). Further, δS at the top of the growing layer is a function of h and the background salt gradient. δT and δS must be such that the water column is stable (i.e., $R_p \geq 1$), yielding the relationship $\delta T \sim h$ (see (8)). The heat content of a layer (HC_L) can thus be related to the layer thickness as follows: $HC_L \propto \delta T h \sim h^2$. Since the model setup is such that lower layers are generally subject to higher heat fluxes than upper layers (see section 2.1), layer thicknesses decrease with height in the staircase.

While the thickness distribution of all layers above the first is similar for all values of τ (Figure 5b), we find that larger τ yields thicker lower layers (Figure 5c). These thick bottom layers are a result of more rapid bottom layer mergers due to the relatively larger salt fluxes compared to heat fluxes for larger τ , which leads to a more rapid reduction of R_p across an interface. As a result of these thick lower layers caused by more efficient merging, staircases have larger mean layer thicknesses at larger values of τ (Figure 5d).

In the Arctic Ocean, it appears in general that the staircase in the Eurasian Basin, subject to generally higher mixing levels than the staircase in the Canadian Basin, exhibits somewhat larger layer thicknesses (see Shibley et al., 2017; see also Kelley, 1984, who examines mean layer thicknesses in oceanic staircases). In addition, a mixed-layer thickness variation with height is prevalent across both Arctic basins (Shibley et al., 2017). Here we show an example from the Canadian Basin from a yearlong ITP observational record, where mixed layers at the top of the staircase are $\approx 10\%$ as thick as layers toward its bottom (Figure 6a); layer thicknesses, calculated according to the procedure outlined in Shibley et al. (2017), increase by 1.2 ± 0.1 m for every 10-m increase in depth in the staircase (Figure 6b). It is important to note that the thick, lower layers we discuss in the observations should not be conflated with thick layers originating from horizontal intrusions where diffusive convection is not the only mechanism in play (e.g., Bebieva & Timmermans, 2017).

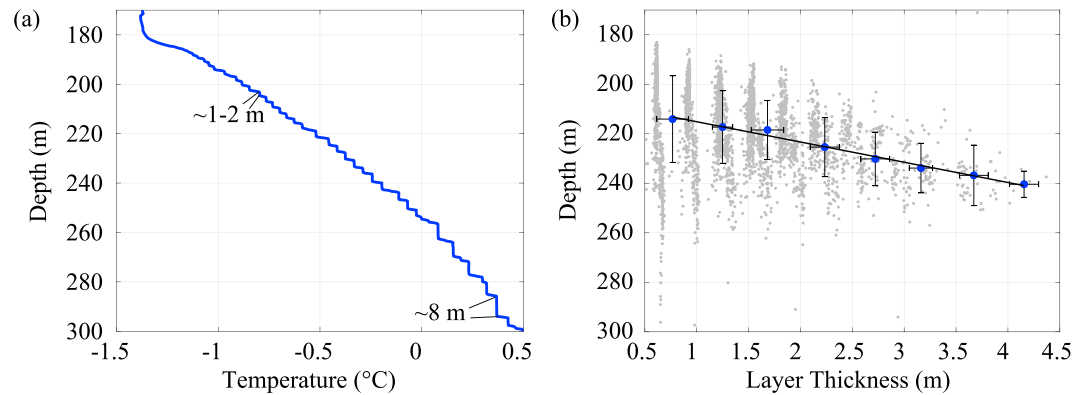


Figure 6. Ice-Tethered Profiler (ITP) measurements in the Canadian Basin. (a) Representative ITP profile (from location CB in Figure 2d) of depth (meters; variables are now dimensional) versus temperature ($^{\circ}\text{C}$) showing mixed layers becoming thicker with depth. (b) ITP measurements of depth (m) versus staircase mixed-layer thicknesses (m), gray dots. Layer thicknesses were calculated following the procedure given by Shibley et al. (2017). Data were binned in 0.5-m increments, and the average depth and mixed-layer thickness in each bin was calculated (blue dots). Error bars indicate ± 1 standard deviation on the binned values. The linear trend (with 95% confidence interval) indicates mixed-layer thicknesses increase by 1.2 ± 0.1 m for every 10-m increase in depth in the staircase. A total of 368 profiles from the yearlong record (August 2007–2008) of ITP 13 were used here. This general observation parallels the results of the 1-D model.

In general, therefore, the layer thickness variation with height that characterizes the Arctic Ocean staircase is consistent with the 1-D model. This suggests that the evolution of the Arctic staircase may be described as a 1-D process where the warm Atlantic water layer approximates an unchanging, bottom heat source. The layer thickness variation is caused by the combination of layers growing into a stable salinity gradient subject to reduced heat fluxes with height in the staircase. In the 1-D model, a variation with heat fluxes in height is an artifact of the model setup (i.e., a system subject to a constant bottom heat flux that is also growing in temperature). In the Arctic setting, such vertical flux divergences may be related to the lateral advection of heat (e.g., Timmermans et al., 2008). The gradient in heat fluxes with height is what is ultimately responsible for the variation in layer thickness with height. For larger values of intermittent turbulence (larger τ), the larger variation in layer thickness, which we attribute to be a result of larger salt fluxes relative to heat fluxes, may be associated with increased merging of layers at the bottom of the staircase in an Arctic setting (for a full analysis of such coarsening, see Radko, 2007).

4.4. Model Result 3: Heat Fluxes

For the same value of R_{ρ} , model results suggest that heat fluxes across interfaces are smaller for larger values of τ within the same regime (Figures 7a and 7b). This interesting and perhaps nonintuitive result may be explained by considering the model formalism. Consider τ_1 and τ_2 , such that $\tau_1 > \tau_2$. The heat flux F_H into an interface boundary layer may be written as $F_H = HC/\Delta t$, where HC is the boundary layer heat content, and Δt is the duration of the boundary layer growth (prior to instability). The boundary layer Rayleigh number Ra_{bl} depends on both the density difference $\delta\rho$ across the boundary layer and the boundary layer thickness, d_{ρ} , as $Ra_{bl} \propto \delta\rho d_{\rho}^3$. d_{ρ} is the following function of Δt and τ : $d_{\rho} \sim (1 - \tau^{1/2})\Delta t^{1/2}$ (see equation (2.16) of Linden & Shirtcliffe, 1978, who show how the thickness of the density boundary layer is related to the thickness of the temperature and salinity boundary layers). Then, the assumption that Ra_{bl} at instability equals a critical Rayleigh number yields $\Delta t_2/\Delta t_1 = [(1 - \tau_1^{1/2})/(1 - \tau_2^{1/2})]^{3/2}$, for constant R_{ρ} . Further, relating the heat content in the boundary layer to both its thickness and the temperature step across it yields the following relationship: $HC \propto \delta T d_{\rho} \sim \Delta t(1 - \tau^{1/2})$, for this diffusive boundary layer. This then shows $HC_2/HC_1 = [(1 - \tau_1^{1/2})/(1 - \tau_2^{1/2})]^{1/2}$. Comparing the relationships between $\Delta t_2/\Delta t_1$ and HC_2/HC_1 indicates that the time necessary to reach boundary layer overturn in a larger- τ case grows faster than does the increased heat content in the boundary layer due to the larger thermal transfer in the presence of intermittent turbulence. The same reasoning applies for both $R_{\rho} \leq \tau^{-1/2}$ (Linden & Shirtcliffe, 1978) and $R_{\rho} > \tau^{-1/2}$ (Newell, 1984) regimes. In each case, all of the heat contained in the boundary layer is removed when it overturns. The net result is that heat fluxes are smaller for larger values of $\tau \leq \tau_c$ in a given regime. For example, for $Q = 0.03$ and $\sigma = 7$, when turbulence is introduced to a level such that $P_T \approx 0.3\%$ (corresponding to $\tau = 0.03$), heat fluxes are reduced by 25% compared to the quiescent case ($\tau = 0.01$) for

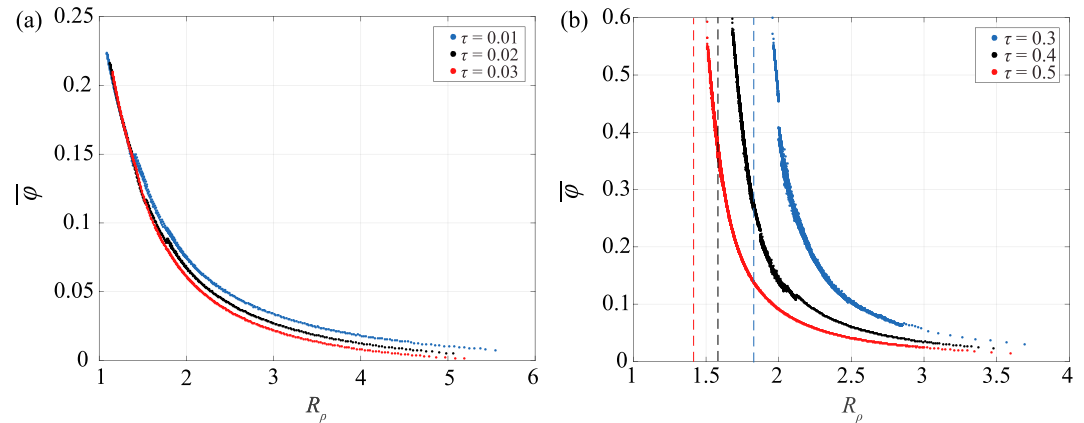


Figure 7. Average dimensionless heat flux versus R_ρ for three values of τ in (a) the Linden and Shirtcliffe (1978) regime at each time step from $t = 0$ to 2,500 (the approximate time at which $\tau = 0.03$ first exits the regime of Linden & Shirtcliffe, 1978), and three values of τ in (b) the Newell (1984) regime at each time step from $t = 0$ to 10,000 (the entire model run). Heat fluxes are taken over the second and third interfaces in the staircase and averaged over every five values of R_ρ . Values of τ at which the system changes from the $R_\rho \leq \tau^{-1/2}$ regime to the $R_\rho > \tau^{-1/2}$ regime are shown by the dashed lines; the line color corresponding to the value of τ is shown in the legend.

$R_\rho = 2.5$ (Figure 7a). Further, for $P_T \approx 12\%$ (corresponding to $\tau = 0.5$), heat fluxes are reduced by 60% compared to when $P_T \approx 5\%$ ($\tau = 0.3$) for $R_\rho = 2.5$ (Figure 7b). We note that even for small levels of turbulent mixing (e.g., $P_T \approx 5\%$), diffusive and convective fluxes at most interfaces are out of balance with each other (i.e., in the Newell (1984) regime, $R_\rho > \tau^{-1/2}$) for the entire evolution of the staircase.

The interplay between diffusive convection and shear-driven turbulence affects heat fluxes in a way that may seem counterintuitive. To exemplify this, we consider four modes of heat transport, for the same background temperature and salinity gradients, that arise from different mixing processes: (1) F_M , the heat flux across a linear gradient driven by molecular fluxes, (2) F_T , the heat flux across a linear gradient driven by turbulent fluxes, (3) $F_{DD,M}$, the heat flux through a diffusive-convective staircase in a quiescent environment, and (4) $F_{DD,T}$, the heat flux through a diffusive-convective staircase in an intermittently turbulent environment. Considering a representative temperature profile in the Canada Basin (see Figure 2a) yields (1) $F_M \approx O(0.01)$ W/m², with $\kappa_T = 10^{-7}$ m²/s; (2) $F_T \approx 0.5$ W/m², using an effective thermal diffusivity of $O(10^{-5})$ m²/s (Bebieva & Timmermans, 2016); and (3) $F_{DD,M} \approx O(0.1)$ W/m², according to estimates of diffusive-convective fluxes from 4/3-flux laws (see, e.g., Shibley et al., 2017). Further, we have shown here that $F_{DD,T}$ tends to be lower than $F_{DD,M}$, for ($\tau \leq \tau_c$). This results in the following relationship: $F_M < F_{DD,T} < F_{DD,M} < F_T$, indicating the complex, and possibly counterintuitive, interconnection between double-diffusive and turbulent processes.

5. Summary and Discussion

Motivated by Arctic Ocean observations, which show that well-formed diffusive-convective staircases are present in the interior Arctic Basin but absent around its boundaries, we examine how intermittent turbulence affects the formation and evolution of the diffusive-convective staircase. We further consider the influence of intermittent turbulence on vertical heat fluxes through the staircase. We find that there is a critical level of intermittent turbulence (i.e., τ_c corresponding to a relative percentage of time P_T that mixing is dominated by shear-driven turbulence) above which a staircase cannot form. Additionally, we find that there is a variation in layer thickness with height in the staircase, which appears to be more pronounced in the presence of intermittent turbulence because relatively high salt fluxes compared to heat fluxes lead to more efficient layer merging. The final main result is that for a fixed value of R_ρ , when turbulence is sufficiently weak to allow for the formation of a staircase, heat fluxes are smaller for stronger turbulence (characterized by larger τ). Thus, increased intermittent turbulence inhibits the transport of heat via diffusive convection.

In the context of Arctic observations, results here suggest lower heat fluxes through staircases in regions subject to larger levels of intermittent turbulence, provided that the level of turbulence has not disrupted the staircase entirely (see Figure 2d). This is a finding that is challenging to validate observationally given the

difficulties of quantifying turbulence levels in a double-diffusive staircase (Guthrie et al., 2017; McDougall & Ruddick, 1992; Padman & Dillon, 1989; Padman, 1994). As discussed previously here in section 1.3, results of Padman (1994) suggest that a sheared staircase may have higher heat fluxes. On the other hand, recent microstructure analyses from a region of the Amundsen Basin indicate a subtle relationship between shear-driven turbulence and active double diffusion, with possibly lower heat fluxes in a weakly turbulent diffusive-convective setting (Guthrie et al., 2015, 2017). Results raise the obvious question of how diffusive-convective fluxes inhibited by turbulence may manifest as variations to the bulk structure of the Atlantic water layer staircase. It may be that the generally thicker mixed layers and stronger bulk vertical temperature gradient characterizing the Eurasian Basin staircase (in contrast to the Canadian Basin staircase) are an indication of higher turbulent mixing levels. Further observational and modeling studies are needed to elucidate the relationship between intermittent turbulence and heat fluxes.

While the 1-D modeling exercise presented here has provided useful insight into the conditions for diffusive-convective staircase formation, structure, and fluxes, it is clear that a 1-D description of the Arctic Ocean staircase is not sufficient (see, e.g., Bebieva & Timmermans, 2017; Timmermans et al., 2008). Future work will require analyses that extend beyond the 1-D framework. Ultimately, we envision the influence of turbulence on a double-diffusive staircase can be sufficiently well characterized that a description of bulk staircase characteristics (e.g., mixed-layer thicknesses) may be useful in constraining the level of shear-driven turbulence in a given setting. A further natural extension of this study is a consideration of diffusive-convective staircase formation in the presence of a steady shear, which would test the limits of our findings on intermittent turbulence. An understanding of how turbulence affects staircase formation and diffusive-convective fluxes may become increasingly relevant in a changing Arctic subject to higher wind-driven mixing as sea ice continues to retreat.

Acknowledgments

The Ice-Tethered Profiler data were collected and made available by the Ice-Tethered Profiler Program (Krishfield et al., 2008; Toole et al., 2011) based at the Woods Hole Oceanographic Institution (<http://www.whoi.edu/itp>). We are grateful for support and useful scientific discussions associated with the Forum for Arctic Modeling and Observational Synthesis (FAMOS) and the FAMOS School for early career Arctic scientists. Nicole Shibley was supported by the Department of Defense (DoD) through the National Defense Science and Engineering Graduate Fellowship (NDSEG) Program. Funding from the National Science Foundation Division of Polar Programs under award 1350046 is also acknowledged.

References

- Bebieva, Y., & Timmermans, M. L. (2016). An examination of double-diffusive processes in a mesoscale eddy in the Arctic Ocean. *Journal of Geophysical Research: Oceans*, *121*, 457–475. <https://doi.org/10.1002/2015JC011105>
- Bebieva, Y., & Timmermans, M. L. (2017). The relationship between double-diffusive intrusions and staircases in the Arctic Ocean. *Journal of Physical Oceanography*, *47*(4), 867–878. <https://doi.org/10.1175/JPO-D-16-0265.1>
- Carmack, E., Polyakov, I., Padman, L., Fer, I., Hunke, E., Hutchings, J., et al. (2015). Toward quantifying the increasing role of oceanic heat in sea ice loss in the new Arctic. *Bulletin of the American Meteorological Society*, *96*(12), 2079–2105. <https://doi.org/10.1175/BAMS-D-13-00177.1>
- Carpenter, J., Sommer, T., & Wüest, A. (2012a). Simulations of a double-diffusive interface in the diffusive convection regime. *Journal of Fluid Mechanics*, *711*, 411–436. <https://doi.org/10.1017/jfm.2012.399>
- Carpenter, J., Sommer, T., & Wüest, A. (2012b). Stability of a double-diffusive interface in the diffusive convection regime. *Journal of Physical Oceanography*, *42*(5), 840–854. <https://doi.org/10.1175/JPO-D-11-0118.1>
- Dewey, R., Muench, R., & Gunn, J. (1999). Mixing and vertical heat flux estimates in the Arctic Eurasian Basin. *Journal of Marine Systems*, *21*(1), 199–205. [https://doi.org/10.1016/S0924-7963\(99\)00014-7](https://doi.org/10.1016/S0924-7963(99)00014-7)
- Dillon, T. M. (1982). Vertical overturns: A comparison of Thorpe and Ozmidov length scales. *Journal of Geophysical Research*, *87*(C12), 9601–9613. <https://doi.org/10.1029/JC087iC12p09601>
- Gargett, A. E. (2003). Differential diffusion: An oceanographic primer. *Progress in Oceanography*, *56*(3), 559–570. [https://doi.org/10.1016/S0079-6611\(03\)00025-9](https://doi.org/10.1016/S0079-6611(03)00025-9)
- Guthrie, J. D., Fer, I., & Morison, J. (2015). Observational validation of the diffusive convection flux laws in the Amundsen Basin, Arctic Ocean. *Journal of Geophysical Research: Oceans*, *120*, 7880–7896. <https://doi.org/10.1002/2015JC010884>
- Guthrie, J. D., Fer, I., & Morison, J. H. (2017). Thermohaline staircases in the Amundsen Basin: Possible disruption by shear and mixing. *Journal of Geophysical Research: Oceans*, *122*, 7767–7782. <https://doi.org/10.1002/2017JC012993>
- Huppert, H. E. (1971). On the stability of a series of double-diffusive layers. *Deep Sea Research and Oceanographic Abstracts*, *18*(10), 1005–1021. [https://doi.org/10.1016/0011-7471\(71\)90005-2](https://doi.org/10.1016/0011-7471(71)90005-2)
- Huppert, H. E., & Linden, P. (1979). On heating a stable salinity gradient from below. *Journal of Fluid Mechanics*, *95*(3), 431–464. <https://doi.org/10.1017/S0022112079001543>
- Inoue, R., Yamazaki, H., Wolk, F., Kono, T., & Yoshida, J. (2007). An estimation of buoyancy flux for a mixture of turbulence and double diffusion. *Journal of Physical Oceanography*, *37*(3), 611–624. <https://doi.org/10.1175/JPO2996.1>
- Kelley, D. (1984). Effective diffusivities within oceanic thermohaline staircases. *Journal of Geophysical Research*, *89*(C6), 10,484–10,488. <https://doi.org/10.1029/JC089iC06p10484>
- Kelley, D., Fernando, H., Gargett, A., Tanny, J., & Özsoy, E. (2003). The diffusive regime of double-diffusive convection. *Progress in Oceanography*, *56*(3), 461–481. [https://doi.org/10.1016/S0079-6611\(03\)00026-0](https://doi.org/10.1016/S0079-6611(03)00026-0)
- Krishfield, R., Toole, J., Proshutinsky, A., & Timmermans, M. L. (2008). Automated ice-tethered profilers for seawater observations under pack ice in all seasons. *Journal of Atmospheric and Oceanic Technology*, *25*(11), 2091–2105. <https://doi.org/10.1175/2008JTECHO587.1>
- Kunze, E. (1990). The evolution of salt fingers in inertial wave shear. *Journal of Marine Research*, *48*(3), 471–504. <https://doi.org/10.1357/002224090784984696>
- Kwok, R., & Untersteiner, N. (2011). The thinning of Arctic sea ice. *Physics Today*, *64*(4), 36–41. <https://doi.org/10.1063/1.3580491>
- Lenn, Y. D., Wiles, P., Torres-Valdes, S., Abrahamson, E., Rippeth, T., Simpson, J., et al. (2009). Vertical mixing at intermediate depths in the Arctic boundary current. *Geophysical Research Letters*, *36*, L05601. <https://doi.org/10.1029/2008GL036792>

- Linden, P., & Shirtcliffe, T. (1978). The diffusive interface in double-diffusive convection. *Journal of Fluid Mechanics*, 87(03), 417–432. <https://doi.org/10.1017/S002211207800169X>
- McDougall, T. J., & Ruddick, B. R. (1992). The use of ocean microstructure to quantify both turbulent mixing and salt-fingering. *Deep Sea Research Part A: Oceanographic Research Papers*, 39(11), 1931–1952. [https://doi.org/10.1016/0198-0149\(92\)90006-F](https://doi.org/10.1016/0198-0149(92)90006-F)
- Merryfield, W. J. (2000). Origin of thermohaline staircases. *Journal of Physical Oceanography*, 30(5), 1046–1068. [https://doi.org/10.1175/1520-0485\(2000\)030<1046:OOTS>2.0.CO;2](https://doi.org/10.1175/1520-0485(2000)030<1046:OOTS>2.0.CO;2)
- Neal, V. T., Neshyba, S., & Denner, W. (1969). Thermal stratification in the Arctic Ocean. *Science*, 166(3903), 373–374. <https://doi.org/10.1126/science.166.3903.373>
- Newell, T. (1984). Characteristics of a double-diffusive interface at high density stability ratios. *Journal of Fluid Mechanics*, 149, 385–401. <https://doi.org/10.1017/S0022112084002718>
- Padman, L. (1994). Momentum fluxes through sheared oceanic thermohaline steps. *Journal of Geophysical Research*, 99(C11), 22,491–22,499. <https://doi.org/10.1029/94JC01741>
- Padman, L., & Dillon, T. M. (1987). Vertical heat fluxes through the Beaufort Sea thermohaline staircase. *Journal of Geophysical Research*, 92(C10), 10,799–10,806. <https://doi.org/10.1029/JC092iC10p10799>
- Padman, L., & Dillon, T. M. (1988). On the horizontal extent of the Canada Basin thermohaline steps. *Journal of Physical Oceanography*, 18(10), 1458–1462. [https://doi.org/10.1175/1520-0485\(1988\)018<1458:OTHEOT>2.0.CO;2](https://doi.org/10.1175/1520-0485(1988)018<1458:OTHEOT>2.0.CO;2)
- Padman, L., & Dillon, T. M. (1989). Thermal microstructure and internal waves in the Canada Basin diffusive staircase. *Deep Sea Research Part A: Oceanographic Research Papers*, 36(4), 531–542. [https://doi.org/10.1016/0198-0149\(89\)90004-6](https://doi.org/10.1016/0198-0149(89)90004-6)
- Polyakov, I. V., Pnyushkov, A. V., Rember, R., Ivanov, V. V., Lenn, Y. D., Padman, L., & Carmack, E. C. (2012). Mooring-based observations of double-diffusive staircases over the Laptev sea slope*. *Journal of Physical Oceanography*, 42, 95–109. <https://doi.org/10.1175/2011JPO4606.1>
- Radko, T. (2003). A mechanism for layer formation in a double-diffusive fluid. *Journal of Fluid Mechanics*, 497, 365–380. <https://doi.org/10.1017/S0022112003006785>
- Radko, T. (2005). What determines the thickness of layers in a thermohaline staircase? *Journal of Fluid Mechanics*, 523, 79–98. <https://doi.org/10.1017/S0022112004002290>
- Radko, T. (2007). Mechanics of merging events for a series of layers in a stratified turbulent fluid. *Journal of Fluid Mechanics*, 577, 251–273. <https://doi.org/10.1017/S0022112007004703>
- Radko, T. (2013). *Double-diffusive convection*. Cambridge, UK: Cambridge University Press.
- Radko, T. (2016). Thermohaline layering in dynamically and diffusively stable shear flows. *Journal of Fluid Mechanics*, 805, 147–170. <https://doi.org/10.1017/jfm.2016.547>
- Radko, T., Flanagan, J., Stellmach, S., & Timmermans, M. L. (2014). Double-diffusive recipes. Part II: Layer-merging events. *Journal of Physical Oceanography*, 44(5), 1285–1305. <https://doi.org/10.1175/JPO-D-13-0156.1>
- Rippeth, T. P., Lincoln, B. J., Lenn, Y. D., Green, J. M., Sundfjord, A., & Bacon, S. (2015). Tide-mediated warming of Arctic halocline by Atlantic heat fluxes over rough topography. *Nature Geoscience*, 8(3), 191–194. <https://doi.org/10.1038/NGEO2350>
- Schmitt, R. W. (1994). Double diffusion in oceanography. *Annual Review of Fluid Mechanics*, 26, 255–285. <https://doi.org/10.1146/annurev.fl.26.010194.001351>
- Shaw, W. J., & Stanton, T. P. (2014). Vertical diffusivity of the Western Arctic Ocean halocline. *Journal of Geophysical Research: Oceans*, 119, 5017–5038. <https://doi.org/10.1002/2013JC009598>
- Shibley, N. C., Timmermans, M. L., Carpenter, J. R., & Toole, J. M. (2017). Spatial variability of the Arctic Ocean's double-diffusive staircase. *Journal of Geophysical Research: Oceans*, 122, 980–994. <https://doi.org/10.1002/2016JC012419>
- Sirevaag, A., & Fer, I. (2012). Vertical heat transfer in the Arctic Ocean: The role of double-diffusive mixing. *Journal of Geophysical Research*, 117, C07010. <https://doi.org/10.1029/2012JC007910>
- Skeel, R., & Berzins, M. (1990). A method for the spatial discretization of parabolic equations in one space variable. *SIAM Journal on Scientific and Statistical Computing*, 11(1), 1–32. <https://doi.org/10.1137/0911001>
- St. Laurent, L., & Schmitt, R. W. (1999). The contribution of salt fingers to vertical mixing in the North Atlantic tracer release experiment*. *Journal of Physical Oceanography*, 29(7), 1404–1424. [https://doi.org/10.1175/1520-0485\(1999\)029<1404:TCOSFT>2.0.CO;2](https://doi.org/10.1175/1520-0485(1999)029<1404:TCOSFT>2.0.CO;2)
- Thorpe, S. A. (1977). Turbulence and mixing in a Scottish loch. *Philosophical Transactions of the Royal Society of London A: Mathematical, Physical, and Engineering Sciences*, 286(1334), 125–181. <https://doi.org/10.1098/rsta.1977.0112>
- Timmermans, M. L., Garrett, C., & Carmack, E. (2003). The thermohaline structure and evolution of the deep waters in the Canada Basin, Arctic Ocean. *Deep Sea Research Part I: Oceanographic Research Papers*, 50(10–11), 1305–1321.
- Timmermans, M. L., Toole, J., Krishfield, R., & Winsor, P. (2008). Ice-Tethered Profiler observations of the double-diffusive staircase in the Canada Basin thermocline. *Journal of Geophysical Research*, 113, C00A02. <https://doi.org/10.1029/2008JC004829>
- Toole, J. M., Krishfield, R. A., Timmermans, M. L., & Proshutinsky, A. (2011). The Ice-Tethered Profiler: Argo of the Arctic. *Oceanography*, 24(3), 126–135. <https://doi.org/10.5670/oceanog.2011.64>
- Turner, J. (1965). The coupled turbulent transports of salt and heat across a sharp density interface. *International Journal of Heat and Mass Transfer*, 8(5), 759–767. [https://doi.org/10.1016/0017-9310\(65\)90022-0](https://doi.org/10.1016/0017-9310(65)90022-0)
- Turner, J. (1968). The behaviour of a stable salinity gradient heated from below. *Journal of Fluid Mechanics*, 33(1), 183–200. <https://doi.org/10.1017/S0022112068002442>
- Turner, J. (2010). The melting of ice in the Arctic Ocean: The influence of double-diffusive transport of heat from below. *Journal of Physical Oceanography*, 40(1), 249–256. <https://doi.org/10.1175/2009JPO4279.1>
- Turner, J., & Stommel, H. (1964). A new case of convection in the presence of combined vertical salinity and temperature gradients. *Proceedings of the National Academy of Sciences*, 52(1), 49–53. <https://doi.org/10.1073/pnas.52.1.49>
- Veronis, G. (1965). On finite amplitude instability in thermohaline convection. *Journal of Marine Research*, 23, 1–17.
- Wells, M., & Griffiths, R. (2003). Interaction of salt finger convection with intermittent turbulence. *Journal of Geophysical Research*, 108, C33080. <https://doi.org/10.1029/2002JC001427>
- Worster, M. G. (2004). Time-dependent fluxes across double-diffusive interfaces. *Journal of Fluid Mechanics*, 505, 287–307. <https://doi.org/10.1017/S0022112004008523>